

TP53 Mutation Spectrum in Breast Cancer Is Subtype Specific and Has Distinct Prognostic Relevance

Laxmi Silwal-Pandit^{1,2}, Hans Kristian Moen Vollaer^{1,2,3}, Suet-Feung Chin^{5,8}, Oscar M. Rueda^{5,8}, Steven McKinney^{10,11}, Tomo Osako^{10,11}, David A. Quigley^{1,2,9}, Vessela N. Kristensen^{1,2,4}, Samuel Aparicio^{10,11}, Anne-Lise Børresen-Dale^{1,2}, Carlos Caldas^{5,6,7,8}, and Anita Langerød^{1,2}

Abstract

Purpose: In breast cancer, the *TP53* gene is frequently mutated and the mutations have been associated with poor prognosis. The prognostic impact of the different types of *TP53* mutations across the different molecular subtypes is still poorly understood. Here, we characterize the spectrum and prognostic significance of *TP53* mutations with respect to the PAM50 subtypes and integrative clusters (IC).

Experimental Design: *TP53* mutation status was obtained for 1,420 tumor samples from the METABRIC cohort by sequencing all coding exons using the Sanger method.

Results: *TP53* mutations were found in 28.3% of the tumors, conferring a worse overall and breast cancer-specific survival [HR = 2.03; 95% confidence interval (CI), 1.65–2.48, $P < 0.001$], and were also found to be an independent marker of poor prognosis in estrogen receptor-positive cases (HR = 1.86; 95% CI, 1.39–2.49, $P < 0.001$). The mutation spectrum of *TP53* varied between the breast cancer subtypes, and individual alterations showed subtype-specific association. *TP53* mutations were associated with increased mortality in patients with luminal B, HER2-enriched, and normal-like tumors, but not in patients with luminal A and basal-like tumors. Similar observations were made in ICs, where mutation associated with poorer outcome in IC1, IC4, and IC5. The combined effect of *TP53* mutation, *TP53* LOH, and *MDM2* amplification on mortality was additive.

Conclusion: This study reveals that *TP53* mutations have different clinical relevance in molecular subtypes of breast cancer, and suggests diverse roles for *TP53* in the biology underlying breast cancer development. *Clin Cancer Res*; 20(13); 1–12. ©2014 AACR.

Authors' Affiliations: ¹Department of Genetics, Institute for Cancer Research, Oslo University Hospital Radiumhospitalet; ²The K.G. Jebsen Center for Breast Cancer Research, Institute for Clinical Medicine, Faculty of Medicine; ³Division of Cancer Medicine, Surgery and Transplantation, Department of Oncology, Oslo University Hospital, Oslo; ⁴Division of Medicine, Department of Clinical Molecular Oncology, Akershus University Hospital, Lørenskog, Norway; ⁵Cancer Research UK, Cambridge Institute; ⁶Cambridge Experimental Cancer Medicine Centre; ⁷Cambridge Breast Unit, Addenbrooke's Hospital, Cambridge University Hospital NHS Foundation Trust and NIHR Cambridge Biomedical Research Centre; ⁸Department of Oncology, University of Cambridge, Cambridge, United Kingdom; ⁹Helen Diller Family Comprehensive Cancer Center, University of California at San Francisco, San Francisco, California; ¹⁰Department of Pathology and Laboratory Medicine, University of British Columbia; and ¹¹Molecular Oncology, British Columbia Cancer Research Center, Vancouver, Canada

Note: Supplementary data for this article are available at Clinical Cancer Research Online (<http://clincancerres.aacrjournals.org/>).

L. Silwal-Pandit and H.K.M. Vollaer share first authorship of this article.

Corresponding Authors: Anita Langerød, Oslo University Hospital, Ulernchausseen 70, Montebello, 0310 Oslo, Norway. Phone: 47-22781376; Fax: 47-22781395; E-mail: anita.langerod@rr-research.no; Anne-Lise Børresen-Dale, Oslo University Hospital, Ulernchausseen 70, Montebello, 0310 Oslo, Norway. E-mail: a.l.borresen-dale@medisin.uio.no; and Carlos Caldas, Cancer Research UK, Cambridge Research Institute, Li Ka Shing Centre, Robinson Way, Cambridge, CB2 0RE, United Kingdom; E-mail: Carlos.Caldas@cruk.cam.ac.uk

doi: 10.1158/1078-0432.CCR-13-2943

©2014 American Association for Cancer Research.

Introduction

Three decades of research on TP53 have documented its fundamental role as a regulator of key cellular processes involved in controlling proliferation and in maintaining the integrity and stability of the genome (2–4). The TP53 tumor suppressor protein is activated in response to a variety of stress signals and suppresses cellular transformation by triggering cell-cycle arrest, DNA repair, and apoptosis. In addition, a role for TP53 in processes such as metabolism, fertility, angiogenesis, immune responses, and stem cell maintenance has been shown (4).

The importance of TP53 in tumor progression is evidenced by the high mutation frequency found in many cancer types, including breast cancer. Point mutations are the most common somatic aberration, followed by small insertions and deletions. The mutations are mostly missense and are predominantly located in exons 5–8, spanning the DNA-binding domain of the protein (5). Mutations may cause complete or partial loss of protein function, acquisition of dominant negative effect, or gain of function (GOF; refs. 6, 7). In addition to mutations, the TP53 pathway may also be disrupted by allelic deletions (Loss of heterozygosity; LOH) of *TP53* or amplification of the TP53 regulator *MDM2*.

Translational Relevance

Somatic mutation in the *TP53* gene is a strong prognostic marker in breast cancer, but the clinical and biologic impact in subtypes has not been clear due to small patient cohorts, suboptimal methods to assess mutation status, and lack of subtyping by molecular profiling. The current study presents analyses of somatic *TP53* mutations in 1,420 patients with breast cancer from the METABRIC (Molecular Taxonomy of Breast Cancer International Consortium) cohort (1), and is the largest to date exploring the effect of *TP53* mutations in a subtype-specific manner. The study shows that the *TP53* mutational spectrum and the prognostic implications indeed are subtype specific. This knowledge is crucial with respect to the potential clinical application of *TP53* as a prognostic and predictive marker, for optimal design of clinical trials, and in further development of *TP53*-targeted therapies.

On the basis of differential gene expression, breast cancer can be classified into five subgroups (luminal A, luminal B, basal-like, HER2-enriched, and normal-like) with distinct biology and clinical outcome (8, 9). These subtypes (PAM50) have been reproduced in several independent studies (10–12). An important development in clinical implementation is the recent recognition of the relevance of subtypes, as implemented in the St. Gallen International Breast Cancer Guidelines, and the development of single sample predictors to classify individual tumors (Nanostring Technologies; ref. 13). As clinical outcome even within subtypes is variable, a more refined taxonomy of breast cancer is still needed. Recently, copy number and gene expression data from 2,000 patients with breast cancer from the METABRIC (Molecular Taxonomy of Breast Cancer International Consortium) cohort were published (1). Integrative clustering of the top 1,000 *cis*-driven genes identified ten subtypes (integrative clusters; IC) with distinct genomic drivers and clinical outcome (14).

Around 30% of breast cancers have been reported to harbor a somatic mutation in the *TP53* gene. *TP53* mutation status is a strong marker of prognosis, while its predictive value is debated (15, 16). Small clinical cohorts, suboptimal methods used to assess *TP53* mutations status, and lack of consistency in how the mutations are classified, have hindered a robust correlation with clinical features (15–18). The frequency and type of mutations vary across the PAM50 subtypes, but the clinical impact is unclear (11, 19, 20). Investigating the association of *TP53* mutations both with PAM50 and the recently described ICs is therefore important.

Here, we report somatic *TP53* mutations in 1,420 patients with breast cancer from the METABRIC cohort and show that both mutational spectrum and prognostic associations are subtype specific. The differences are discussed in relation to important biologic features, such as *TP53* LOH, *MDM2*

amplification, genomic instability, mutational process, and evolutionary selection in the tumor. The overall aim of the study was to create a more solid fundament for clinical trial design and for future implementation of *TP53* as a biomarker.

Materials and Methods

Patient material

TP53 mutation status was successfully obtained for 1,420 tumor samples from the METABRIC cohort (1). Detailed inclusion/exclusion criteria are shown in the patient flow diagram (Supplementary Fig. S1). The fresh-frozen specimens from primary invasive breast carcinomas before adjuvant treatment were collected from five different sites in the United Kingdom and Canada after ethical committee approval (Addenbrooke's Hospital, Cambridge, United Kingdom; Guy's Hospital, London; Nottingham; Vancouver; Manitoba), along with clinical and pathologic annotation. The mean age was 60.5 years at the time of diagnosis/surgery (range 21.9–96.3 years) and mean follow-up was 7.6 years (range 0.1–24.5 years). The Kaplan–Meier plots were truncated at 15 years.

Sequencing analysis

Extraction of nucleic acids was performed as previously described (1). *TP53* mutation status was assessed by sequencing the entire coding region (exons 2–11), including splice junctions. The sequencing was performed according to the manufacturer's procedures using BigDye Terminator v1.1 Cycle Sequencing Kit (Life Technologies), which applies the Sanger sequencing chemistry. The samples were run on the 3730 DNA Analyzer (Life Technologies), a capillary electrophoresis-based automated DNA sequencer.

The sequences had been previously analyzed automatically, which underestimated mutation calls (1). Therefore, here the electropherograms were inspected manually, assisted by the SeqScape v2.5 software (Life Technologies), by two experienced operators. Any discrepancies in mutation calls were resolved by resequencing the samples.

The probability of occurrence of a mutation was estimated for each exon separately in samples with all exons successfully sequenced. Samples with one or more exons unsuccessfully sequenced and no mutations detected were excluded from analysis if the probability of having a mutation was >5% ($n = 22$). Patients with double mutations ($n = 7$) were excluded from the statistical analyses due to the uncertain contribution of each mutation. These 29 samples were not included in the final 1,420 dataset. Survival analysis included 1,404 patients due to patients lost to follow-up ($n = 16$).

Mutation classification

The mutations were classified according to predicted effect on the protein (16); missense in DNA-binding motif (DBM), missense outside DBM, and nonmissense mutations (including splice, inframe, frameshift, and nonsense mutations).

Molecular subclassification and genomic instability scoring

Subtype assignment (PAM50 and IC) was done as described previously (1). Copy number (Affymetrix SNP 6.0) and expression data (Illumina HT 12_v3) are deposited at the European Genome-Phenome Archive (EGA, <http://www.ebi.ac.uk/ega/>) under accession number EGAS00000000083.

Scoring of genomic instability from SNP6 data was performed using different approaches. The Complex Arm Aberration Index (CAAI) captures short genomic regions with highly complex rearrangements such as firestorms (21). Genomic Instability Index (GII) is the proportion of amplified or deleted genomic loci (22). *TP53* and *APO-BEC3B* expression levels were measured using the ILMN_1779356 and ILMN_2219466 probes, respectively. Allele-specific copy number analysis of tumors, which corrects for tumor percentage and ploidy, was used to score allele-specific copy number of *TP53* and *MDM2* (23).

Lymphocyte infiltration and TP53 IHC scoring

The degree of lymphocytic infiltration was assessed in samples with adequate morphology on hematoxylin and eosin-stained fresh-frozen tissue sections (1,105/1,420 samples). The tumors were classified as "absent" (no infiltration), "mild" (light scattering of lymphoid cells), or "severe" (dense infiltration of lymphoid cells forming confluent sheets).

TP53 immunostaining was performed using a monoclonal antibody (clone DO-7, dilution 1:100; Dako) on 4- μ m thick formalin-fixed paraffin-embedded (FFPE) tissue microarray (TMA) sections. The labeling index value was evaluated by discretizing the percentage (1%–100%) of positive nuclei within the invasive portion of each core of the TMA. A total of 869 cases had intact cores with sufficient tumor cells for *TP53* scoring.

Statistical analysis

All statistical analysis were performed using R (24) with the package "rms" (25) and SPSS 18.0 software (SPSS Inc.). Pearson's chi-squared (χ^2), Fisher's exact test, *t*-test, or Kruskal–Wallis test were used when appropriate to test association between different variables. Breast cancer-specific survival (BCSS), defined as the time of diagnosis to the time of a breast cancer-related death, and overall survival (OS), defined as the time of diagnosis to the time of death from any cause, were used for the survival analyses. The Kaplan–Meier estimator with log-rank test for significance and Cox proportional hazard (PH) models were used for the survival analysis. Inspection of standard log–log plots and tests based on correlation between time and Schoenfeld's partial residuals was used to evaluate violations of the assumption of PH in the multivariate models (26).

Results

Characterization of TP53 mutations

TP53 was mutated in 28.3% ($n = 402$) of 1,420 cases (Supplementary Table S1). The majority of the mutations

were single base substitutions ($n = 295$, 73.4%), followed by small deletions ($n = 75$, 18.7%) and insertions ($n = 21$, 5.2%). Complex mutations, comprising both deletions and insertions, ($n = 8$, 2.0%) and tandem mutations ($n = 3$, 0.7%) were uncommon. Eight (2.7%) of the base substitutions were silent/synonymous and were considered wild-type in further analyses, giving a total mutation frequency of 27.7% ($n = 394$). The single base substitutions ($n = 287$; silent excluded) were predominantly G:C>A:T transitions ($n = 142$, 49.5%), frequently at CpG sites (88/142, 62%), and A:T>T:A transversions were least common ($n = 13$, 4.5%). The proportion of G:C>A:T at CpG sites was highest in tumors with basal-like phenotype (Supplementary Fig. S2).

The distribution of the mutations was nonuniform across the gene with 81% of the mutations clustering in exons 5–8, mostly spanning the DNA-binding domain of the protein. Exons 4 and 10 also harbored a substantial number of mutations, with 9.6% and 6.5% of the total count, respectively. Only 2% of the mutations were in exon 9, and the remaining 1% was in exons 2, 3, and 11 (Fig. 1 and Supplementary Table S1). Alterations at putative splice sites (defined here as two nucleotides before and after an exon) were detected in 17 cases, and the majority resided between exons 5 and 8. Mutational hotspots (5) were observed in codons 175, 179, 196, 213, 245, 248, 273, 278, 285, and 306. The mutations were mostly G:C>A:T transitions, which in codons 196, 213, and 306 resulted in nonsense codons due to the specific sequence context.

Interestingly, frameshift mutations were evenly distributed along the gene with no hotspots, whereas missense, nonsense (both with several hotspots), inframe, and splice mutations were mainly located in the DNA-binding domain (Fig. 1 and Supplementary Table S1). Several types of mutations, including a cluster of missense mutations, hit the oligomerization domain; these potentially prevent the formation of tetramers. Nonsense and missense mutations were nearly mutually exclusive with respect to hotspot mutational sites. This observation cannot solely be explained by codon context. The high mutability of C to T, likely followed by selection may explain this pattern.

A systematic overview of the consequences of different types of *TP53* mutations on both mRNA and protein expression in a large cohort of breast cancer is currently not available. Hence, we stratified the tumors by mutation status, and found a high correlation between *TP53* mRNA levels and protein expression, but only in mutated tumors ($P < 0.001$, Kruskal–Wallis test; Supplementary Fig. S3B). Tumors with missense mutations were predominantly IHC positive and had higher mRNA levels, whereas frameshift and nonsense mutations were predominantly IHC negative with lower mRNA levels (Supplementary Fig. S3A and S3B). Half of the wild-type tumors also showed positive IHC, but the staining intensity was relatively weak and not correlated with mRNA levels. These results show that IHC is an inadequate surrogate method for mutation screening.

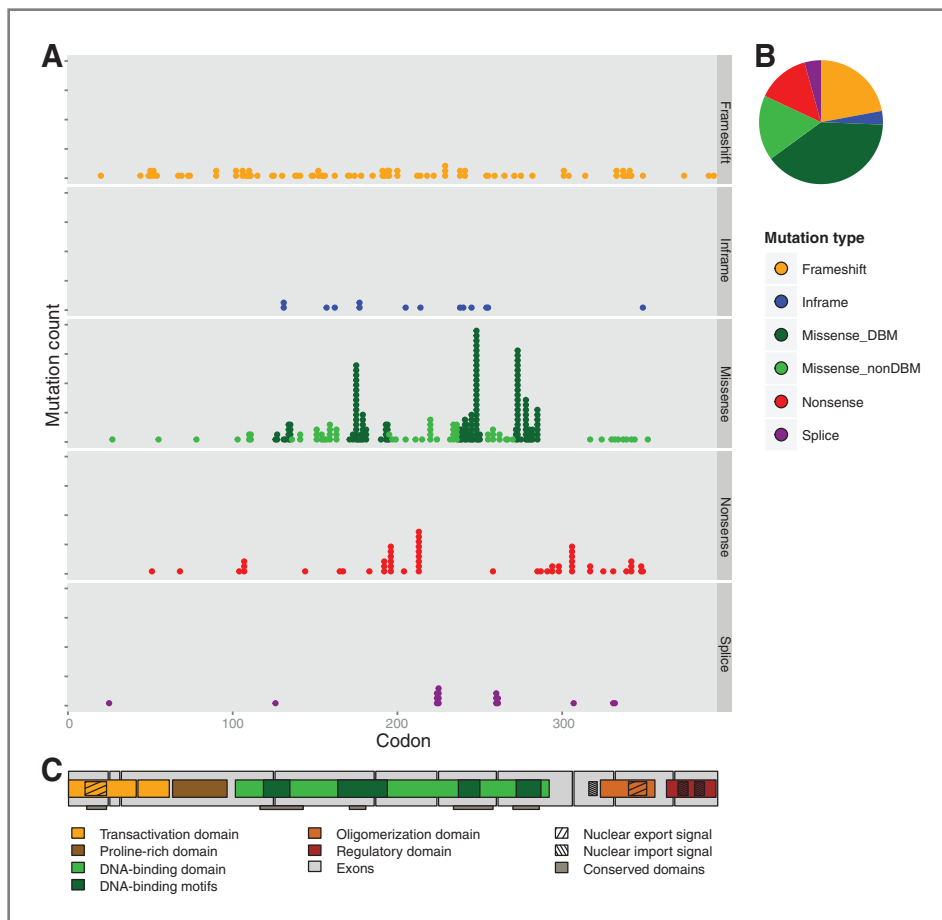


Figure 1. *TP53* mutation spectrum in breast cancer. A, distribution of mutation type across the gene. B, pie chart showing the fraction of each mutation category. C, conserved and functional domains of *TP53*.

Spectrum of *TP53* mutations in molecular subtypes

TP53 mutations were differentially distributed in PAM50 subtypes ($P < 0.001$, χ^2 test; Table 1), which confirms previous reports (11, 19). The subtypes with high mutation frequency, basal-like (65%), and HER2-enriched (53%) showed enrichment of nonmissense mutations, whereas the luminal B type showed a high proportion of missense mutations, of which the majority affected the DBM ($P = 0.061$, χ^2 test; Fig. 2A, 2C, and 2D).

A notable difference of mutational hotspots was observed between subtypes. The basal-like subtype was enriched for multiple hotspots, whereas luminal A tumors had a flat mutation profile. The most frequently mutated codon 248, was identified as a hotspot in luminal B, HER2-enriched, and basal-like tumors, whereas mutations in codon 175 and 273 were observed mostly in the basal-like subgroup. Interestingly, the nonsense mutation R213* was a hotspot in basal-like (seven out of nine samples; Fig. 2A and 2B). This intriguing finding is also observed in other cohorts, where 16 of 20 samples with the R213* mutation are basal-like (data not shown).

The distribution of *TP53* mutations in the 10 ICs also revealed significant variation in frequency ($P < 0.001$, χ^2 test; Table 1). IC10 had the highest mutation frequency (76.5%), and the mutational spectrum observed in basal-

like tumors was recapitulated (Fig. 2B), suggesting association with the core basal-like subset (14). The proportion of IC9 tumors (48%) with *TP53* mutations is noteworthy because this cluster primarily consists of estrogen receptor (ER)-positive/HER2-negative cases. The distribution of *TP53* mutations across the 10 clusters was validated in The Cancer Genome Atlas (TCGA) dataset by performing analysis of deviance. This confirmed IC9, an ER-positive/HER2-negative subtype, as frequently mutated (Supplementary Fig. S4).

We observed that high *APOBEC3B* expression level was associated with *TP53* mutations ($P < 0.001$, t -test). Interestingly, this effect was strongest in the basal-like tumors (Supplementary Fig. S5), suggesting a subtype-related mechanism contributing to *TP53* mutagenesis. The DNA cytosine deaminase *APOBEC3B* has recently been suggested as a driver of mutations, especially C-to-T and C-to-G substitutions at TC motifs with nonmethylated cytosines, and was shown to be overexpressed in *TP53*-mutated cell lines and tumors (27).

Prognostic implications of *TP53* mutations in breast cancer

Patients with breast cancer with a somatic *TP53* mutation had significantly inferior BCSS [HR = 2.03; 95% confidence

Table 1. Association between TP53 mutation status and clinicopathological characteristics (n = 1,420)

Characteristics		wt TP53	mut TP53	P value ^a
		No. (%)	No. (%)	
Age (years)	≤55	320 (65.7)	167 (34.3)	<0.001
	>55	706 (75.7)	227 (24.3)	
	Missing	0		
Type	Ductal	748 (67.8)	356 (32.2)	<0.001
	Lobular	99 (92.5)	8 (7.5)	
	IDC + ILC	64 (86.5)	10 (13.5)	
	Tubular	59 (92.2)	5 (7.8)	
	Mucinous	37 (97.4)	1 (2.6)	
	Medullary	10 (47.6)	11 (52.4)	
	Other invasive	9 (75.0)	3 (25.0)	
	Missing	0		
Tumor size	T1 (≤2 cm)	456 (75.4)	149 (24.6)	0.06
	T2 (>2–≤5 cm)	515 (69.7)	224 (30.3)	
	T3 (>5 cm), T4	51 (73.9)	18 (26.0)	
	Missing	7		
Node status	Neg (pN0)	539 (75.3)	177 (24.7)	0.011
	Pos (pN1–pN3)	483 (69.1)	216 (30.9)	
	Missing	5		
Grade	1	119 (95.2)	6 (4.8)	<0.001
	2	479 (88.7)	61 (11.3)	
	3	383 (54.5)	320 (45.5)	
	Missing	52		
Estrogen receptor	Pos	906 (82.3)	195 (17.7)	<0.001
	Neg	120 (37.6)	199 (62.4)	
	Missing	0		
Progesteron receptor ^b	Pos	627 (84.4)	116 (15.6)	<0.001
	Neg	399 (58.9)	278 (41.1)	
	Missing	0		
HER2 ^b	Gain	184 (57.9)	134 (42.1)	<0.001
	Loss/balanced	840 (76.6)	257 (23.4)	
	Missing	5		
TP53 LOH ^c	Yes	403 (56.4)	312 (43.6)	<0.001
	No	611 (89.2)	74 (10.8)	
	Missing	20		
MDM2 amplification ^c	Yes	311 (61.6)	194 (38.4)	<0.001
	No	693 (80.4)	169 (19.6)	
	Missing	53		
PAM50	Basal-like	82 (35.0)	152 (65.0)	<0.001
	HER2-enriched	75 (46.6)	86 (53.4)	
	Luminal B	285 (75.2)	94 (24.8)	
	Luminal A	460 (90.7)	47 (9.3)	
	Normal-like	121 (89.0)	15 (11.0)	
	Missing	3		
IC10	IC1	83 (77.6)	24 (22.4)	<0.001
	IC2	43 (79.6)	11 (20.4)	
	IC3	192 (93.7)	13 (6.3)	
	IC4	207 (83.1)	42 (16.9)	
	IC5	64 (46.4)	74 (53.6)	
	IC6	41 (63.1)	24 (36.9)	
	IC7	114 (87.0)	17 (13.0)	

(Continued on the following page)

Table 1. Association between *TP53* mutation status and clinicopathological characteristics ($n = 1,420$) (Cont'd)

Characteristics	wt <i>TP53</i>		mut <i>TP53</i>		P value ^a
	No.	(%)	No.	(%)	
Adjuvant therapy	IC8	191 (93.2)	14 (6.8)		
	IC9	52 (52.0)	48 (48.0)		
	IC10	39 (23.5)	127 (76.5)		
	Missing	0			
	CT	9 (29.0)	22 (71.0)		<0.001
	CT/RT	45 (34.4)	86 (65.6)		
	CT/HT/RT	99 (69.7)	43 (30.3)		
	CT/HT	19 (73.1)	7 (26.9)		
	HT	245 (81.4)	56 (18.6)		
	HT/RT	375 (78.9)	100 (21.1)		
	RT	110 (71.9)	43 (28.1)		
	None	124 (77.0)	37 (23.0)		
	Missing	0			

^aPearson's χ^2 or Fisher's exact test (two-tailed) when 2×2.

^bProgesteron status defined by gene expression data. HER2 status defined by SNP6 data.

^c*TP53* LOH and *MDM2* gain defined by SNP6 data (not corrected for ploidy).

interval (CI), 1.65–2.48, $P < 0.001$, Cox Regression model; Fig. 3A and Supplementary Table S2] and OS (HR = 1.59; 95% CI, 1.34–1.89, $P < 0.001$; Supplementary Fig. S6A). *TP53* mutations were associated with increased mortality also in the subset of patients that did not receive cytotoxic treatment ($n = 1,078$, HR = 2.20; 95% CI, 1.69–2.86, $P < 0.001$; Supplementary Fig. S6B), which suggests that the effect is not related to response of adjuvant chemotherapy. Importantly, stratification of cases showed that the prognostic effect of *TP53* was limited to ER-positive disease (Fig. 3C and D). As ER-positive and -negative breast cancers are widely recognized as different biologic entities, separate multivariate survival analyses were performed. After correcting for other covariates, *TP53* mutation status was an independent predictor of outcome in ER-positive patients only, both for BCSS (HR = 1.86; 95% CI, 1.39–2.49, $P < 0.001$; Supplementary Table S3) and for OS (HR = 1.49; 95% CI, 1.17–1.90, $P < 0.001$; Supplementary Table S4).

The large number of cases allowed survival analysis stratified by molecular subtypes. *TP53* mutations were associated with a worse outcome in luminal B (HR = 1.66; 95% CI, 1.14–2.42, $P = 0.007$), HER2-enriched (HR = 1.69; 95% CI, 1.04–2.73, $P = 0.032$), and normal-like subtypes (HR = 3.62; 95% CI, 1.67–7.88, $P = 0.001$), whereas no significant effect was observed in the basal-like and luminal A subtypes (Fig. 4). *TP53* mutations conferred higher mortality in IC1 (HR = 2.00; 95% CI, 1.01–3.95, $P = 0.045$), IC4 (HR = 2.08; 95% CI, 1.19–3.63, $P = 0.009$), and IC5 (HR = 1.88; 95% CI, 1.13–3.14, $P = 0.015$), although the number of events limits the statistical robustness of these results (Supplementary Fig. S7). IC10 corresponds mostly to triple-negative cases from the basal-like

subtype (1, 14), and no prognostic effect was observed in this highly *TP53*-mutated (76.5%) group. Taken together these novel observations indicate that the clinical significance of mutant *TP53* varies across molecular subtypes of breast cancer.

Survival differences could not be detected in patients harboring different types of *TP53* mutations (Fig. 3B). Although patients with tumors bearing missense mutations in the DBM tended to have inferior outcome, this was not statistically significant.

***TP53* and genomic instability**

TP53 mutation is associated with genomic instability (28). *TP53*-mutated tumors had significantly higher rate of GII ($P < 0.001$, Kruskal–Wallis test), most distinct in basal-like cases. Focal complex alterations are believed to be associated with telomeric attrition and a result of breakage-fusion-bridge cycles, and suggest a different mechanism for instability of the genome (21, 29). Higher rates of these complex alterations (firestorms), measured by CAAI, were observed in mutated tumors ($P < 0.001$, χ^2 test; predominantly in the basal-like and HER2-enriched subgroups).

We further investigated whether tumors acquire genomic instability through alternative mechanisms of the *TP53* pathway deregulation (*TP53* LOH and *MDM2* amplification). Significantly higher frequencies of *TP53* LOH and *MDM2* amplification were observed in mutated versus wild-type tumors ($P < 0.001$, χ^2 test; Table 1), with no clear association with the type of mutation. LOH was observed in 80.8% of the mutated tumors, independently of molecular subtype. However, in *TP53* wild-type cases, the frequency of LOH varied across subtypes ($P < 0.001$, χ^2 test); 52% in luminal B versus 24% in basal-like (Supplementary

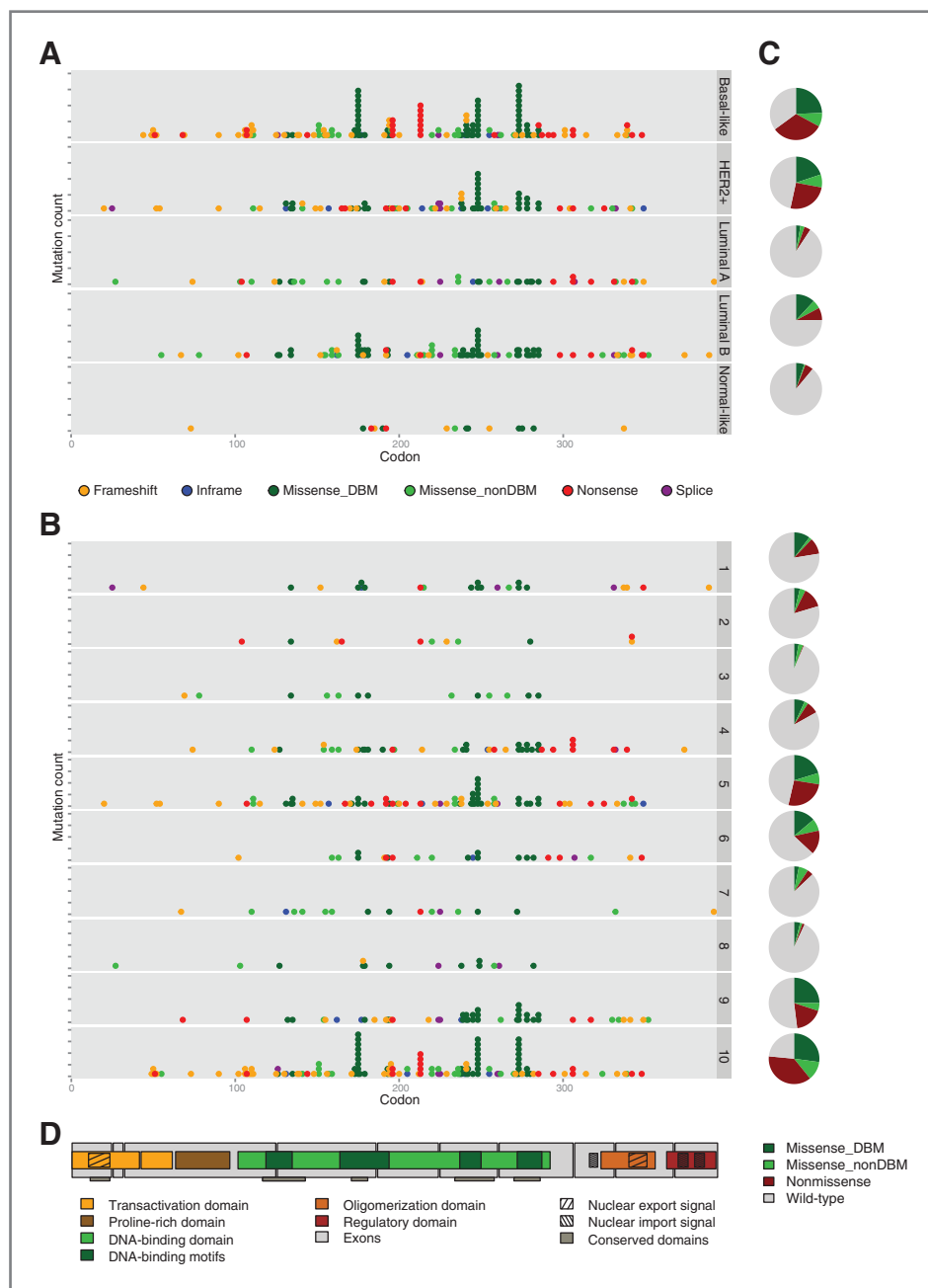


Figure 2. *TP53* mutation spectrum in molecular subtypes. A, PAM50 and (B) IC subtypes. C, pie chart showing fraction of mutation type in each subtype. D, conserved and functional domains of *TP53*.

Fig. S8A). The difference was even more prominent across ICs; 80% in IC1 compared with 35% in IC10 (Supplementary Fig. S8A). These alternative mechanisms of the *TP53* pathway deregulation increased the mortality in patients with wild-type tumors (LOH vs. no LOH: HR = 1.56; 95% CI, 1.20–2.02, $P < 0.001$; *MDM2* amplification vs. no *MDM2* amplification: HR = 1.86; 95% CI, 1.43–2.42, $P < 0.001$), but not in patients with mutated *TP53* (Supplementary Fig. S8B). Interestingly, the combined influence of these events (*TP53* mutation, *TP53* LOH, or *MDM2* amplification) conferred increasingly unfavorable progn-

osis (HR = 1.54; 95% CI, 1.39–1.70, $P < 0.001$; Fig. 5A) and tumors showed correspondingly higher genomic instability ($P < 0.001$, Kruskal–Wallis test; Fig. 5B).

Discussion

The current study presents analyses of somatic *TP53* mutations in a large cohort of 1,420 breast cancer cases with extensive clinical and molecular annotation. Our previous study was of significant size ($n = 1794$), but a large proportion of the samples (64%) was only screened

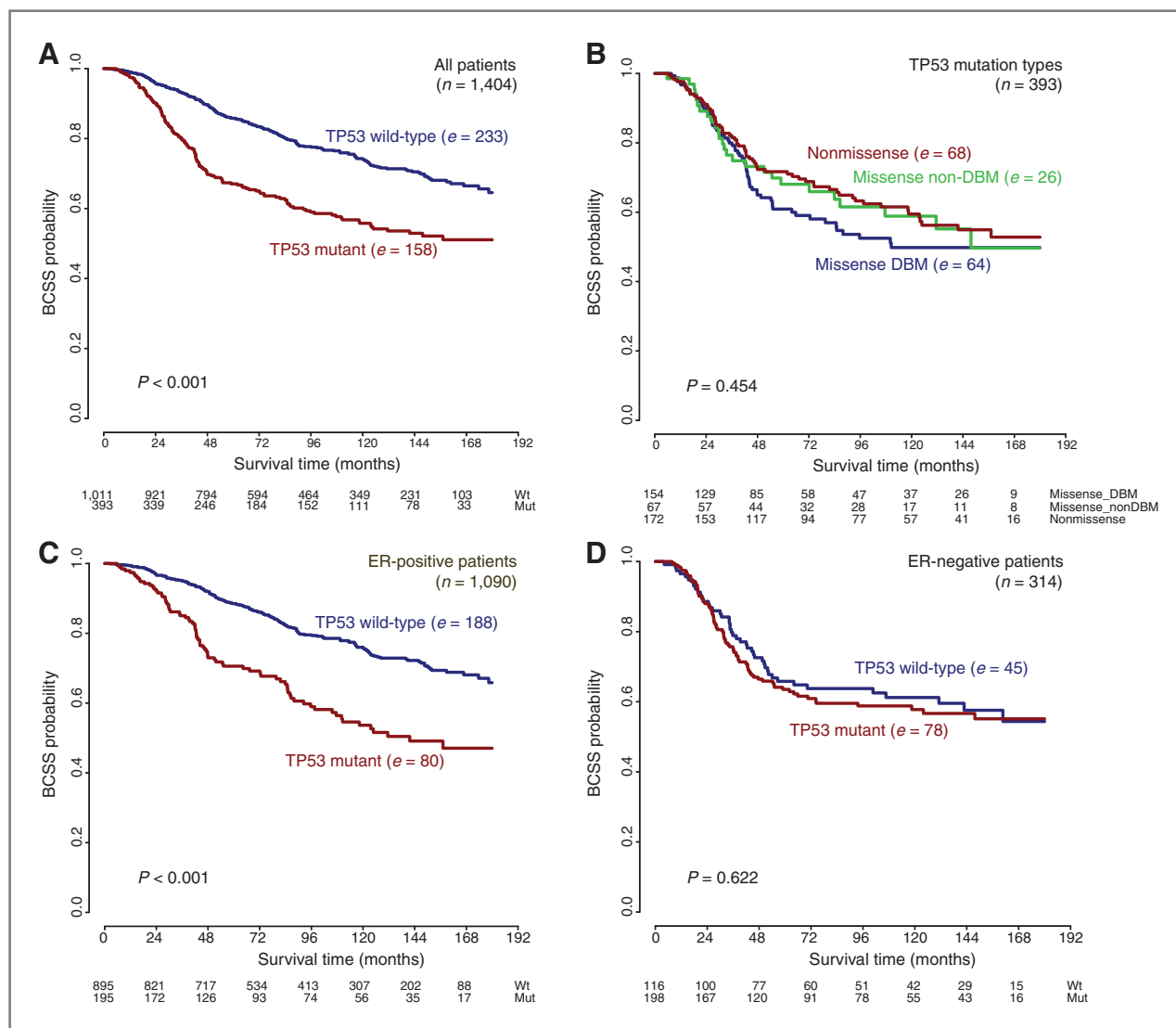


Figure 3. Kaplan-Meier survival curves showing BCSS of *TP53* mutation status in (A) the total cohort, (B) patients categorized according to *TP53* mutation types, (C) ER-positive patients, and (D) ER-negative patients. Numbers at risk are listed below each chart (e = number of breast cancer-specific deaths).

for mutations in exons 5–8 and molecular subtype information was not available (16). The TCGA dataset includes 826 samples with *TP53* mutation status, but survival data are extremely limited (10). This makes METABRIC the largest cohort exploring the effect of *TP53* mutations in breast cancer in a subtype-specific manner. The large sample size allowed FDR correction (data not presented) and the key results presented are therefore robust.

The distribution pattern of *TP53* mutations was is in line with previous studies, with the majority of mutations localized in the DNA-binding domain (exons 5–8). Notably, almost 20% of the mutations were detected outside this domain, and the prognostic significance of these mutations was equivalent to those residing in the DNA-binding domain. This highlights the need to sequence all *TP53* exons to explore its clinical impact.

The distribution of *TP53* mutation types across its functional domains provides insight into the selection processes during tumorigenesis. Frameshift mutations, as opposed to other mutation types, were evenly distributed along the gene (Fig. 1). Thus, selective advantage of mutations in the DNA-binding domain, mirroring the functional importance of this region, does not extend to frameshift mutations. This suggests that frameshift mutations disrupt protein function independently of location.

The impact of the *TP53* mutation types on outcome could be related to the predicted functional effect, although reports of this association have been inconsistent (16, 30–35). In this study, the prognostic impact was not significantly different between mutation types. Missense mutations predicted to have GOF (6, 36) were also not distinctly associated with outcome. The LOH events in *TP53*-mutated tumors were often accompanied by copy

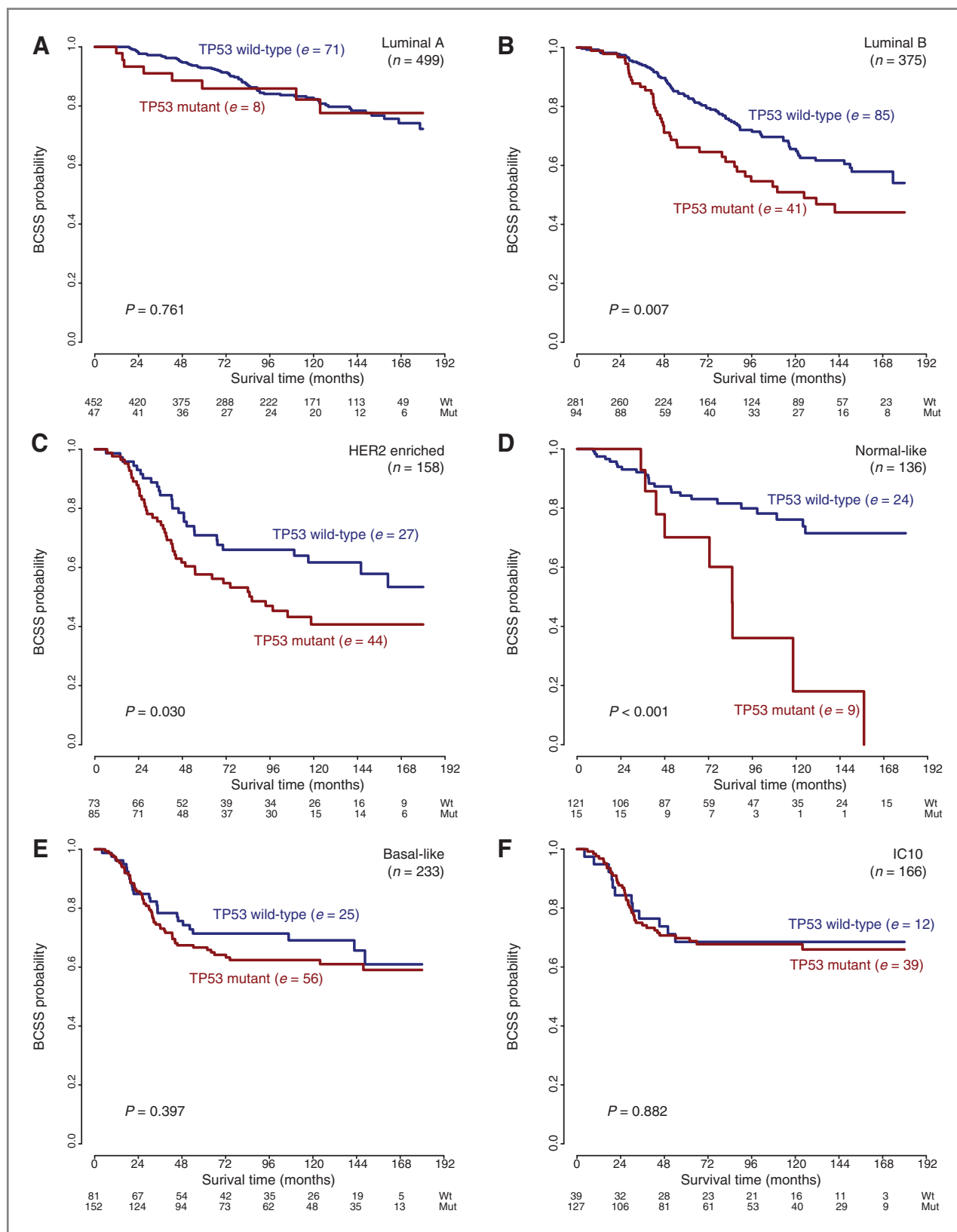


Figure 4. Kaplan-Meier survival curves showing BCSS of TP53 mutation status in PAM50 and IC10 breast cancer subtypes. A, luminal A. B, luminal B. C, HER2-enriched. D, normal-like. E, basal-like. F, IC10. Numbers at risk are listed below each chart (e = no. of breast cancer-specific deaths).

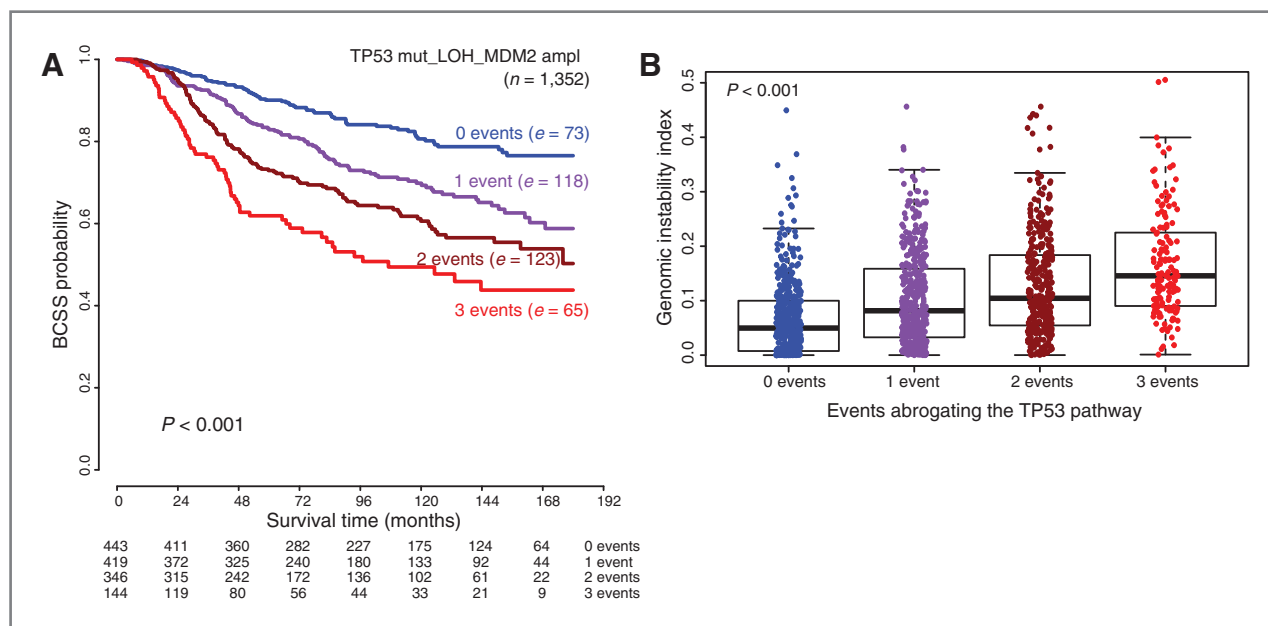


Figure 5. A, Kaplan-Meier survival curves showing BCSS of *TP53* mutation status in combination with both *TP53* LOH and *MDM2* amplification. Numbers at risk are listed below each chart (e = number of breast cancer-specific deaths). B, relation between genomic instability and the *TP53* pathway disrupting events (*TP53* mutation, *TP53* LOH, and *MDM2* gain).

number gain (mostly duplication) of the retained allele. This occurred independently of mutation type, suggesting that allelic duplication does not enhance the effect of GOF-mutant proteins. Altogether, these observations question whether different mutation types, including GOF mutations, can be used as a prognostic tool in breast cancer.

The distinct *TP53* mutation spectrum and clinical relevance across molecular subtypes suggest a diverse role for *TP53*. As seen in previous studies (10, 20), basal-like cancers were frequently mutated and enriched for frameshift and nonsense mutations, but *TP53* mutation was not prognostic. In a recent study, *TP53* function was found to be compromised in most of the basal-like tumors either through *TP53* mutations or alterations in genes in the *TP53* pathway (10). Thus, wild-type *TP53* may not necessarily indicate an intact *TP53* pathway and may explain this lack of prognostic value. Our interpretation is that abrogation of the *TP53* pathway is an early, initiating, and required event in most basal-like tumors. In addition, inactivation of both *TP53* alleles seems to be important in these tumors given the higher proportion of cases with both mutation and LOH (Supplementary Fig. S8A). In ER-negative disease, where both *TP53* and other markers performed poorly in prognostication (Supplementary Table S2–S4), severe lymphocytic infiltration is associated with better outcome (37–39). We observed that ER-negative tumors with wild-type *TP53* and severe lymphocytic infiltration are a subset with better prognosis (Supplementary Fig. S8C). Whether wild-type *TP53* evokes an immune response in ER-negative tumors, or whether the immune response is only effective against wild-type *TP53* tumors needs to be investigated.

Recurrently mutated codons (hotspots) were observed, particularly in basal-like/IC10 tumors. Hotspots probably arise due to a combination of a highly mutable sequence context and selective growth advantage provided by the specific mutation. One intriguing observation was the association of the nonsense mutation in codon 213 (C.R213*) with the basal-like subtype. Codon 213 (CGA/CGG) is a polymorphic site (rs1800372) with G as the minor allele (minor allele frequency = 0.007; ref. 40). The C>T mutation leading to a stop codon is possible only with the A allele (CGA>TGA), indicating a protective role of the G-allele.

Loss of one *TP53* allele may be a sufficient driver in luminal B tumors as indicated by the higher fraction of wild-type tumors with LOH (Supplementary Fig. S8A). A less important role of *TP53* mutation is suggested in luminal A tumors due to the low mutation frequency and lack of evident hotspots.

In conclusion, our integrated study provides an important insight into the significance of *TP53* in breast cancer, clearly demonstrating that its role as a prognostic and predictive marker needs to be investigated in a subtype-specific manner. This knowledge is crucial with respect to the potential clinical application of *TP53*, including further development of *TP53*-targeted therapies.

Disclosure of Potential Conflicts of Interest

No potential conflicts of interest were disclosed.

Authors' Contributions

Conception and design: S. Aparicio, A.-L. Børresen-Dale, C. Caldas, A. Langerød

Development of methodology: L. Silwal-Pandit, A.-L. Børresen-Dale, C. Caldas, A. Langerød

Acquisition of data (provided animals, acquired and managed patients, provided facilities, etc.): S.-F. Chin, T. Osako, C. Caldas

Analysis and interpretation of data (e.g., statistical analysis, biostatistics, computational analysis): L. Silwal-Pandit, H.K. Moen Vollan, S.-F. Chin, O.M. Rueda, S.E. McKinney, D. Quigley, V.N. Kristensen, A.-L. Børresen-Dale, C. Caldas, A. Langerød

Writing, review, and/or revision of the manuscript: L. Silwal-Pandit, H.K. Moen Vollan, S.-F. Chin, S.E. McKinney, D. Quigley, S. Aparicio, A.-L. Børresen-Dale, C. Caldas, A. Langerød

Administrative, technical, or material support (i.e., reporting or organizing data, constructing databases): L. Silwal-Pandit, S.E. McKinney, C. Caldas, A. Langerød

Study supervision: A.-L. Børresen-Dale, C. Caldas, A. Langerød

Acknowledgments

The authors thank the members of the METABRIC group list of members below) for sample collection and for providing the clinical and genomic data on 2,000 breast tumors, the patients who contributed to the study, and

Puong Vu, Anita Halvei, Inger Riise Bergheim, Anja Valen, Rita Halvorsen, Eldri Undlien Due, Jovana Jovanovic, and Shiferaw Dagim Tadele for the efforts to read the sequences of more than 4.2 million bases manually.

Grant Support

This work was supported by Norwegian Cancer Society (0332), South-Eastern Norway Regional Health Authority (2011079), The Research Council of Norway (163027/V40), The Norwegian Radium Hospital Foundation, EuroCan Platform FP7 (260791), The British Columbia Cancer Foundation, and Cancer Research UK.

The costs of publication of this article were defrayed in part by the payment of page charges. This article must therefore be hereby marked *advertisement* in accordance with 18 U.S.C. Section 1734 solely to indicate this fact.

Received October 25, 2013; revised April 25, 2014; accepted April 28, 2014; published OnlineFirst May 6, 2014.

References

- Curtis C, Shah SP, Chin S-F, Turashvili G, Rueda OM, Dunning MJ, et al. The genomic and transcriptomic architecture of 2,000 breast tumours reveals novel subgroups. *Nature* 2012;486:346–52.
- Lane DP, Crawford LV. T antigen is bound to a host protein in SV40-transformed cells. *Nature* 1979;278:261–3.
- Linzer DI, Levine AJ. Characterization of a 54K dalton cellular SV40 tumor antigen present in SV40-transformed cells and uninfected embryonal carcinoma cells. *Cell* 1979;17:43–52.
- Lane D, Levine A. p53 Research: the past thirty years and the next thirty years. *Cold Spring Harb Perspect Biol* 2010;2:a000893.
- Petitjean A, Mathe E, Kato S, Ishioka C, Tavtigian SV, Hainaut P, et al. Impact of mutant p53 functional properties on TP53 mutation patterns and tumor phenotype: lessons from recent developments in the IARC TP53 database. *Hum Mutat* 2007;28:622–9.
- Oren M, Rotter V. Mutant p53 gain-of-function in cancer. *Cold Spring Harb Perspect Biol* 2010;2:a001107.
- Muller PAJ, Vousden KH. p53 mutations in cancer. *Nat Cell Biol* 2013;15:2–8.
- Perou CM, Sørlie T, Eisen MB, van de Rijn M, Jeffrey SS, Rees CA, et al. Molecular portraits of human breast tumours. *Nature* 2000;406:747–52.
- Sørlie T, Perou CM, Tibshirani R, Aas T, Geisler S, Johnsen H, et al. Gene expression patterns of breast carcinomas distinguish tumor subclasses with clinical implications. *Proc Natl Acad Sci U S A* 2001;98:10869–74.
- Cancer Genome Atlas Research Network. Comprehensive molecular portraits of human breast tumours. *Nature* 2012;490:61–70.
- Sørlie T, Tibshirani R, Parker J, Hastie T, Marron JS, Nobel AB, et al. Repeated observation of breast tumor subtypes in independent gene expression data sets. *Proc Natl Acad Sci U S A* 2003;100:8418–23.
- Hu Z, Fan C, Oh DS, Marron JS, He X, Qaqish BF, et al. The molecular portraits of breast tumors are conserved across microarray platforms. *BMC Genomics* 2006;7:96.
- Harbeck N, Sotlar K, Wuerstlein R, Doisneau-Sixou S. Molecular and protein markers for clinical decision making in breast cancer: Today and tomorrow. *Cancer Treat Rev* 2014;40:434–44.
- Dawson S-J, Rueda OM, Aparicio S, Caldas C. A new genome-driven integrated classification of breast cancer and its implications. *EMBO J* 2013;32:617–28.
- Børresen-Dale A-L. TP53 and breast cancer. *Hum Mutat* 2003;21:292–300.
- Olivier M, Langerød A, Carrieri P, Bergh J, Klaar S, Eyfjord J, et al. The clinical value of somatic TP53 gene mutations in 1,794 patients with breast cancer. *Clin Cancer Res* 2006;12:1157–67.
- Alsner J, Jensen V, Kyndi M, Offersen BV, Vu P, Børresen-Dale A-L, et al. A comparison between p53 accumulation determined by immunohistochemistry and TP53 mutations as prognostic variables in tumours from breast cancer patients. *Acta Oncol* 2008;47:600–7.
- Ozcelik H, Pinnaduwage D, Bull SB, Andrulis IL. Type of TP53 mutation and ERBB2 amplification affects survival in node-negative breast cancer. *Breast Cancer Res Treat* 2007;105:255–65.
- Langerød A, Zhao H, Borgan Ø, Nesland JM, Bukholm IRK, Ik Dahl T, et al. TP53 mutation status and gene expression profiles are powerful prognostic markers of breast cancer. *Breast Cancer Res* 2007;9:R30.
- Holstege H, Horlings HM, Velds A, Langerød A, Børresen-Dale A-L, van de Vijver MJ, et al. BRCA1-mutated and basal-like breast cancers have similar aCGH profiles and a high incidence of protein truncating TP53 mutations. *BMC Cancer* 2010;10:654.
- Russnes HG, Vollan HKM, Lingjaerde OC, Krasnitz A, Lundin P, Naume B, et al. Genomic architecture characterizes tumor progression paths and fate in breast cancer patients. *Sci Transl Med* 2010;2:38ra47–7.
- Bilal E, Dutkowskij J, Guinney J, Jang IS, Logsdon BA, Pandey G, et al. Improving Breast Cancer Survival Analysis through Competition-Based Multidimensional Modeling. *PLoS Comput Biol* 2013;9:e1003047.
- Van Loo P, Nordgard SH, Lingjaerde OC, Russnes HG, Rye IH, Sun W, et al. Allele-specific copy number analysis of tumors. *Proc Natl Acad Sci U S A* 2010;107:16910–5.
- R Core Team (2014). R: A language and environment for statistical computing. R Foundation for Statistical Computing, Vienna, Austria. <http://www.R-project.org/>.
- Frank E Harrell Jr (2014). rms: Regression Modeling Strategies. R package version 4.2-0. <http://CRAN.R-project.org/package=rms>.
- Harrell FE. Regression modeling strategies. Springer Verlag; 2001.
- Burns MB, Lackey L, Carpenter MA, Rathore A, Land AM, Leonard B, et al. APOBEC3B is an enzymatic source of mutation in breast cancer. *Nature* 2013;494:366–70.
- Hanel W, Moll UM. Links between mutant p53 and genomic instability. *J Cell Biochem* 2012;113:433–9.
- Hicks JB, Krasnitz A, Lakshmi B, Navin NE, Riggs M, Leiby E, et al. Novel patterns of genome rearrangement and their association with survival in breast cancer. *Genome Res* 2006;16:1465–79.
- Powell B, Soong R, Iacopetta B, Seshadri R, Smith DR. Prognostic significance of mutations to different structural and functional regions of the p53 gene in breast cancer. *Clin Cancer Res* 2000;6:443–51.
- Végran F, Rebucci M, Chevrier S, Cadouet M, Boidot R, Lizard-Nacol S. Only missense mutations affecting the DNA binding domain of p53 influence outcomes in patients with breast carcinoma. *PLoS ONE* 2013;8:e55103.
- Fernández-Cuesta L, Oakman C, Falagan-Lotsch P, Smoth K-S, Quinaux E, Buysse M, et al. Prognostic and predictive value of TP53 mutations in node-positive breast cancer patients treated with anthracycline- or anthracycline/taxane-based adjuvant therapy: results from the BIG 02-98 phase III trial. *Breast Cancer Res* 2012;14:R70.

33. Rossner P, Gammon MD, Zhang Y-J, Terry MB, Hibshoosh H, Memeo L, et al. Mutations in p53, p53 protein overexpression and breast cancer survival. *J Cell Mol Med* 2009;13:3847–57.
34. Børresen-Dale A-L, Andersen TI, Eyfjörd JE, Cornelis RS, Thorlacius S, Borg A, et al. TP53 mutations and breast cancer prognosis: particularly poor survival rates for cases with mutations in the zinc-binding domains. *Genes Chromosomes Cancer* 1995;14:71–5.
35. Overgaard J, Yilmaz M, Guldborg P, Hansen LL, Alsner J. TP53 mutation is an independent prognostic marker for poor outcome in both node-negative and node-positive breast cancer. *Acta Oncol* 2000;39:327–33.
36. Freed-Pastor WA, Mizuno H, Zhao X, Langerød A, Moon S-H, Rodriguez-Barrueco R, et al. Mutant p53 disrupts mammary tissue architecture via the mevalonate pathway. *Cell* 2012;148:244–58.
37. Teschendorff AE, Miremadi A, Pinder SE, Ellis IO, Caldas C. An immune response gene expression module identifies a good prognosis subtype in estrogen receptor negative breast cancer. *Genome Biol* 2007;8:R157.
38. Schmidt M, Böhm D, Törne von C, Steiner E, Puhl A, Pilch H, et al. The humoral immune system has a key prognostic impact in node-negative breast cancer. *Cancer Res* 2008;68:5405–13.
39. Rody A, Holtrich U, Pusztai L, Liedtke C, Gaetje R, Ruckhaeberle E, et al. T-cell metagene predicts a favorable prognosis in estrogen receptor-negative and HER2-positive breast cancers. *Breast Cancer Res* 2009;11:R15.
40. 1000 Genomes Project Consortium Abecasis GR, Altshuler D, Auton A, Brooks LD, Durbin RM, et al. A map of human genome variation from population-scale sequencing. *Nature* 2010;467:1061–73.

Clinical Cancer Research

***TP53* Mutation Spectrum in Breast Cancer Is Subtype Specific and Has Distinct Prognostic Relevance**

Laxmi Silwal-Pandit, Hans Kristian Moen Vollan, Suet-Feung Chin, et al.

Clin Cancer Res Published OnlineFirst May 6, 2014.

Updated version	Access the most recent version of this article at: doi: 10.1158/1078-0432.CCR-13-2943
Supplementary Material	Access the most recent supplemental material at: http://clincancerres.aacrjournals.org/content/suppl/2014/05/07/1078-0432.CCR-13-2943.DC1

E-mail alerts	Sign up to receive free email-alerts related to this article or journal.
Reprints and Subscriptions	To order reprints of this article or to subscribe to the journal, contact the AACR Publications Department at pubs@aacr.org .
Permissions	To request permission to re-use all or part of this article, use this link http://clincancerres.aacrjournals.org/content/early/2014/06/12/1078-0432.CCR-13-2943 . Click on "Request Permissions" which will take you to the Copyright Clearance Center's (CCC) Rightslink site.